Design and Implementation of a Dual Excited Planar Circular Array Antenna for Base Stations

Except where reference is made to the work of others, the work described in this thesis is my own or was done in collaboration with my advisory committee. This thesis does not include proprietary or classified information.

Veneela Ammula

Certificate of Approval:

Prathima Agrawal Professor Electrical and Computer Engineering	Sadasiva M. Rao, Chair Professor Electrical and Computer Engineering
Stuart M. Wentworth Associate Professor Electrical and Computer Engineering	George T. Flowers Dean Graduate School

Design and Implementation of a Dual Excited Planar Circular Array Antenna for Base Stations

Veneela Ammula

A Thesis

Submitted to

the Graduate Faculty of

Auburn University

in Partial Fulfillment of the

Requirements for the

Degree of

Master of Science

Auburn, Alabama
Dec 18, 2009

Design and Implementation of a Dual Excited Planar Circular Array Antenna for Base Stations

Veneela Ammula

Permission is granted to Auburn University to make copies of this thesis at its discretion, upon the request of individuals or institutions and at their expense. The author reserves all publication rights.

Signature of Author

Date of Graduation

Vita

Veneela Ammula, daughter of Raghu Ammula and Padmavathy Ammula was born on September 7^{th}, 1985, in Guntur District, India. She received the Bachelor of Engineering degree in Electrical Engineering from Vasavi college of Engineering in 2007. She joined the Masters program in the Department of Electrical and Computer Engineering at Auburn University in August 2007. Her current area of research is focused on Design of Base Station Array Antennas.

Thesis Abstract

Design and Implementation of a Dual Excited Planar Circular Array Antenna for Base Stations

Veneela Ammula

Master of Science, Dec 18, 2009
(B.E., Osmania University, 2007)

63 Typed Pages

Directed by Sadasiva M. Rao

Smart antennas present a promising solution to the present day capacity and coverage shortage in mobile wireless communications. These intelligent antennas when used at the base station can avoid a lot of interference by transmitting and receiving signals only in desired directions. Circular array antennas have gained popularity among various antenna configurations used for direction agile applications.

The purpose of this thesis is to design a planar circular array antenna for base stations in mobile wireless communication systems. The antenna could be electronically steered to give a complete 360 coverage around the base station. The model was created using FEKO Suite 5.4, a Method of Moments (MoM) based electromagnetic simulation software. Particle Swarm Optimization algorithm was applied to maximize the gain of the antenna in a single azimuth direction. Ideal dimensions for the antenna structure were obtained from the optimization process.

The designed antenna was fabricated and tested in an anechoic chamber to verify its radiation characteristics. The experimental results were found to be in good agreement with the simulation results. An improved design configuration was simulated for future development of this array antenna.

Acknowledgments

First and foremost, I would express my sincere gratitude to my advisor Professor Sadasiva M Rao for his guidance and help during my study and research at Auburn. Thanks for leading me into the research area of wireless communications and antenna design. Without his patience and support, this thesis would not be possible.

I thank Professor Prathima Agrawal for supporting me through a graduate research fellowship which made this work possible.

My thanks also go out to Professor Stuart M Wentworth and Calvin Cutshaw for rendering their professional skills to the completion of the prototype and Professor Lloyd Stephen Riggs for his patient assistance in using the facilities in the Antenna Laboratory.

I would like to again specially thank all my advisory committee members Dr. Sadasiva M. Rao, Dr. Prathima Agarwal and Dr. Stuart M. Wentworth for all the constant support and guidance throughout my studies at Auburn.

I am grateful to my parents for their consistent support and encouragement during my study and thanks to my friends for their kind presence whenever needed.

Style manual or journal used Journal of Approximation Theory (together with the style known as "aums"). Bibliograpy follows van Leunen's *A Handbook for Scholars.*

Computer software used The document preparation package TEX (specifically LATEX) together with the departmental style-file `aums.sty`.

Table of Contents

List of Figures xi

1 Introduction 1
1.1 Evolution of Cellular Network 1
1.1.1 Cell Splitting 3
1.1.2 Cell Sectoring 3
1.2 Smart Antennas 5
1.3 Organization of Thesis 6

2 Design of the Dual Excited Planar Circular Array Antenna 8
2.1 Circular Array Antenna Theory 11
2.1.1 Radiation pattern of a general array 11
2.1.2 Array factor 12
2.1.3 Array pattern 12
2.2 Array Design 13

3 SIMULATION SOFTWARE: FEKO 15
3.1 Method of Moments 16
3.2 FEKO Suite components 17
3.3 Optimization 18
3.3.1 OPTFEKO 18
3.3.2 Particle Swarm Optimization 19
3.4 Simulation of the antenna model in FEKO 20
3.5 Optimal Geometry 23
3.6 Results 24
3.6.1 Observations 26
3.7 Antenna design with improved gain 28
3.7.1 Radiation Patterns 30
3.7.2 Observations 31

4 Fabrication of the Antenna 33
4.1 Feed Network for Antenna Array 35

5 Experimental Verification 40
5.1 Measuring the Resonant Frequency and input impedance 40
5.2 Measuring the gain of the antenna 42
5.3 Results 44

6 Conclusion 47

Bibliography 49

List of Figures

1.1 Cellular system geometry.(Figure obtained from [1]) 2

1.2 Omnidirectional Antenna and Coverage Patterns. 2

1.3 Cell Splitting.(Figure obtained from [3]) 3

1.4 Cell Sectoring. 4

1.5 Sectorised antenna for Base stations. 4

1.6 Comparison of Coverage patterns of different antenna configurations. (Figure from [6]) 7

2.1 An arbitrary array antenna 11

2.2 Geometry of the array antenna. 13

2.3 Geometry of the antenna with only essential elements. 14

3.1 Diverse applications of FEKO software(Figure obtained [11]) 16

3.2 Particle Swarm Optimization as modeled by a swarm of bees searching for flowers (Figure obtained from [13]) 20

3.3 CADFEKO view showing the meshing and far field parameters of the antenna 22

3.4 Parameters for Particle swarm optimization 23

3.5 Geometry of the complete antenna array 24

3.6 Radiation patterns for the antenna 26

3.7 Radiation pattern of antenna 27

3.8 Comparison of radiation patterns for different antenna configurations 28

3.9 Geometry of the new antenna design 29
3.10 Radiation patterns for the new antenna 31
4.1 Top view of the fabricated antenna 33
4.2 Side view of fabricated antenna 34
4.3 Block Diagram of power divider 35
4.4 Wilkinson power divider and it equivalent microstrip line implementation 36
4.5 The transmission parameters of Wilkinson power splitter 37
4.6 Reflection parameters of Wilkinson power splitter 37
4.7 Isolation parameters of Wilkinson power splitter 38
4.8 Fabricated Wilkinson Power Divider 38
4.9 Power Splitter connected to the ports of the antenna 39
5.1 An RF anechoic chamber 41
5.2 SWR measurement of the antenna 42
5.3 DAMS tripod stand (Figure obtained from [12]) 43
5.4 Antenna placed on wooden block for support 44
5.5 Initializing a measurement in DAMS (Figure obtained from [12]) . . . 44
5.6 Radiation pattern in Horizontal plane 45
5.7 The simulated and measured radiation patterns of antenna 45

Chapter 1

Introduction

In recent years there has been an explosive growth in the number of wireless users, particularly in the area of mobile communication. This growth has triggered need for improving the capacity, coverage and quality of service. Researchers are exploring several new technologies to make effective use of the limited resources. Smart antenna technology provides a key to these problems.

1.1 Evolution of Cellular Network

To accommodate all the users in limited available frequencies or the channels a cellular structure has been designed to systematically provide service to the mobile users. In this design, a coverage zone is divided into small hexagonal segments called cells. Fig. 1.1 shows the Cellular system geometry.

Each cell has an omnidirectional antenna located at the center of the cell. Fig. 1.2 shows the radiation pattern of an omnidirectional antenna. Each cell is allotted a set a frequencies which are different from the neighboring cells. The size of the cell is defined by various factors such as the local terrain, the frequency band in which the network operates and capacity requirement in that region.

The same frequencies could be used in different cells provided they are situated at a distance large enough to avoid interference. In Fig. 1.1, the cells with the same alphabetical notation use the same set of frequencies. This is known as *frequency reuse*. The cells are grouped into clusters such that the frequencies allocated to a

Figure 1.1: Cellular system geometry.(Figure obtained from [1])

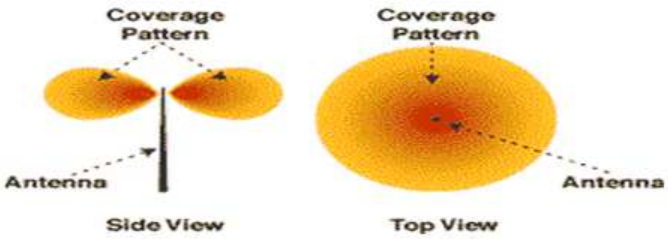

Figure 1.2: Omnidirectional Antenna and Coverage Patterns.

particular cell within a cluster can only be re-used by a corresponding cell in adjacent

clusters. Since each of these cells reuses the frequency spectrum, a significant increase in capacity can be achieved.

1.1.1 Cell Splitting

The cells can be further divided into micro cells to aid the congestion problem as shown in Fig. 1.3. Each of these micro cells is provided with an individual base station with smaller range and less transmission power. This helps in improving the capacity but at the same time it increases the number of hand offs and processing required per user. *Hand off* is a phenomenon of transferring the communication from one base station to another when the mobile user is moving from one cell to another. In cell splitting the radius of the cell R is decreased while maintaining the D/R ratio value to be constant, where D is the distance between the centers of clusters [6].

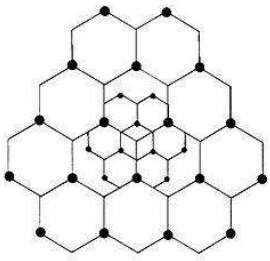

Figure 1.3: Cell Splitting.(Figure obtained from [3])

1.1.2 Cell Sectoring

With further requirement of increased number of channels, cells are divided into regions called *sectors*. Each cell is divided into 3 sectors of 120 degrees each. Fig. 1.4 shows the cellular structure with cells divided into sectors.

In cell sectoring the radius of the cell remains constant decreasing the D/R ratio. Sector antennas limit the direction of radiation by resolving directivity of antenna

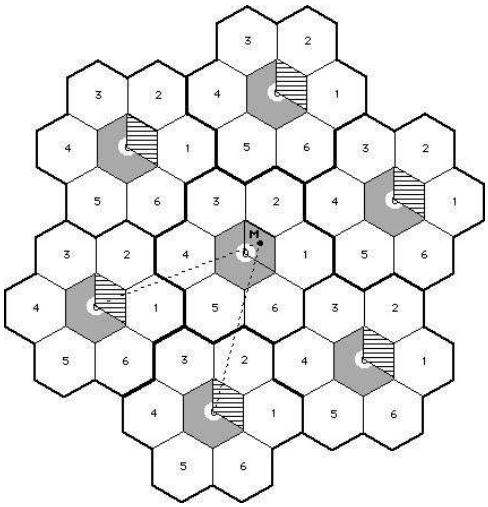

Figure 1.4: Cell Sectoring.

into sectors. Omni directional antennas were replaced by directional antennas such as Monopole Yagi-Uda arrays antennas. Fig. 1.5 shows a sectorised antenna for Base station.

Figure 1.5: Sectorised antenna for Base stations.

Co-channel interference, which is a phenomenon of disturbance or cross talk that occurs when two users in different cells use the same frequency, is greatly reduced in cells which use sector antennas compared to the ones which use omnidirectional antennas. The signal to interference ratio (S/I) increases greatly.

1.2 Smart Antennas

Unlike wireless systems in the past, which used fixed antenna systems, smart antennas or adaptive arrays are dynamically able to adapt to the changing traffic requirements. Smart antennas, usually employed at the base station, radiate narrow beams to serve different users. When the users are well separated spatially the same frequency can be reused, even if the users are in the same cell. This additional intra-cell channel reuse based on spatial separation is the key in achieving an increase in the capacity of the system. So the coverage of smart antennas is greater than the conventional base transceiver station (BTS) antennas.

When smart antenna technology was first introduced in the 1960's it was used in military communication systems, were narrow beams where used in order to avoid interference arising from noise and other jamming signals. Extending the smart antenna concept further, researchers worked on the technology to apply it to the personal communication industry to accommodate more users in the wireless network by suppressing interference.

Smart antenna systems extend cell sectoring by providing coverage to the sector through multiple beams. These multiple beams are obtained by using antenna arrays, where the number of beams covering a sector is determined as a function of array geometry. As they can reject interference in unwanted directions and direct radiation towards the desired user they provide greater coverage for each base station. The capacity of the system is also improved as the bit error rate (BER) is lower. There are two types of smart antennas. They are Switched beam antennas and Adaptive array antennas.

Switched beam forming is a smart antenna approach in its simplest form. Here, multiple fixed beams in predetermined directions are used to serve the users. In

this approach the base station switches between several beams that give the best performance as the mobile user moves through the cell. But the drawback is that if an interferer is present at the center of the directive beam then the undesired user gets enhanced.

Adaptive beam forming is the most advanced approach based on smart antenna techniques. It uses an antenna array backed by strong signal processing capability to automatically change the beam pattern in accordance with the changing signal environment. It directs maximum radiation in the direction of the desired mobile user and also introduces nulls in the interfering directions while tracking the desired mobile user at the same time. The adaptation is achieved by multiplying the incoming signal with complex weights and then summing them together to obtain the desired radiation pattern. These weights are computed to adapt to the changes in the signal environment. The complex weight computation based on different criteria is incorporated in the signal processor in the form of software algorithms. Fig. 1.6 shows the comparison among switched beam systems, adaptive arrays and sector antennas in terms of their coverage in both low interference and high interference environments.

Although better performance is expected in the adaptive array, the switched beam system holds the advantage of being easier to integrate with the current system.

1.3 Organization of Thesis

Chapter 2 starts with the literature review of various antennas proposed for producing directive beams with beam steering properties. The radiation pattern of an arbitrary antenna array is explained. This is followed by an overview of the configuration of the proposed Dual Excited Planar Circular Array Antenna

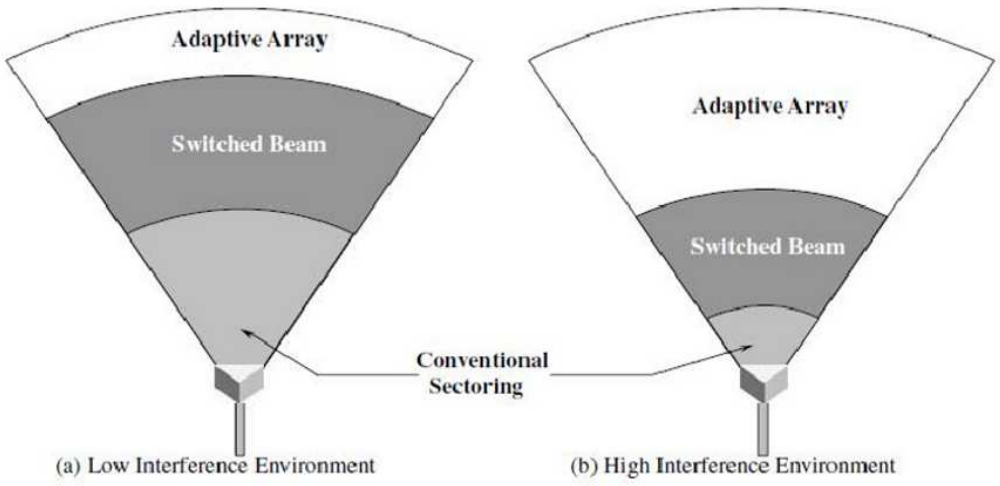

Figure 1.6: Comparison of Coverage patterns of different antenna configurations. (Figure from [6])

Chapter 3 gives a brief introduction to the Electromagnetic simulation software, FEKO. It explains the particle swarm optimization method used in optimizing the dimensions of the model and the methodology followed for simulation of antenna design. The simulation results are also presented along with an improved design for future study.

Chapter 4 explains the fabrication of the antenna structure. It is followed by design and fabrication of a feed network for the antenna which is a Wilkinson power splitter. Performance of the splitter is validated by experimental measurement of its electromagnetic properties.

Chapter 5 deals with the measurements of the radiation pattern characteristics of the fabricated antenna in the anechoic chamber using the help of Desktop Antenna Measurement System.

The thesis is then concluded in Chapter 6 by summarizing the design, fabrication and experimental characterization of the Dual Excited Planar Circular Array Antenna. Ideas for improving the results obtained in this work are also discussed.

Chapter 2

Design of the Dual Excited Planar Circular Array Antenna

The Yagi-Uda antenna array is used for many applications where a narrow beamwidth and high gain is required. Basically, it comprises a driven element, a reflector element placed behind the driven element and at least one director element placed in front. The reflector and director elements are parasitic elements, which when suitably designed,[2] , provide a directive radiation pattern.

Circular arrays have become very popular in mobile and wireless communications because of their advantages over other configurations. They provide symmetry. As they do not have edge elements, directional patterns synthesized with a uniform circular array (UCA) can be electronically steered in 360 degrees without any significant change in the beam shape [16]. Reference [20] compares UCA with uniform rectangular array (URA) and planar uniform circular array (PUCA) antennas to find the best suitable configuration for smart antenna applications. Simulation results showed very good beamformed patterns with PUCAs with deep nulls towards the angles of interference. Of all three geometries, the UCA was shown to have the best patterns with narrowest main beam pointing towards the direction of the signal of interest (SOI). This might be due to the large separation between nearly diametrically opposite elements. When URA and the PUCA antennas with similar areas were compared it was found that slightly greater directivity was obtained when PUCAs were used.

The beam forming properties of circular array antennas have been studied in reference [8]. An array of monopoles arranged along the circular ring on a ground plate was considered. In the first case simulations were done to find the optimum

number of elements that could be accommodated in a circular ring and it was found that a six element array was enough to produce a directive beam in the desired direction. In the second case simulations were carried on to find the effect of different excitation schemes. In this, experiments were conducted by changing the number of excited elements in the array. It was observed that when two element were excited best beam focusing properties were observed in both azimuth and vertical planes. In the third case the radius of the ground plane was varied and the radiation pattern for each configuration has been studied. It was observed that as the radius of the ground plate, Rg, decreased, the angle of elevation of the main beam increased till Rg reached one wavelength and further increase in Rg lowered the elevation of the beam. The antenna was fabricated to compare its results with the simulations and a close match between them was found. The directivity produced in the azimuth plane remained to be 6 dB which requires an improvement.

Various configurations of switched parasitic arrays which could provide angular diversity were proposed in reference [19]. In these designs the signal source remained constant and other surrounding parasitic elements were either short-circuited or open-circuited to provide directive radiation pattern.

Reference [9] presents design of a circular array composed of 25 wire monopole elements. The configuration comprises an element fed with supply positioned at the center of the ground plane. The remaining 24 elements are uniformly dispersed along two concentric rings around the center element. These elements are reactively loaded to change the electrical length of the elements to produce directive beams. By changing the loads a 360 degree beam scan is produced with 30 degree increments. The antenna array was designed to operate at 1 GHz frequency. Manual optimization was performed to find the values for 50 Ω impedance matching and required beam width such that the elements behind the driven element act as reflectors and the ones

in front of it act as directors. To extend operation to other frequencies, optimization should be carried out at each desired frequency and parameters that direct the pattern need to be recalculated. And the manual optimization method followed to find the best values for the parameters is often tedious and may not provide the best optimized values for the considered configuration.

A configuration similar to the above design has been proposed in reference [5] to operate at 2.4 GHz frequency. The configuration consists of an excited element at the center of a hollow cylindrical ground structure and six elements arranged around it in a circle. The elements were loaded at the bottom using varactors to control their reactances and help produce beam patterns in different directions. The ground is chosen to be a hollow cylinder to accommodate the driver circuit and also to reduce the angle of elevation of the radiation pattern. A genetic algorithm has been applied to the antenna configuration using HFSS software to optimize the dimensions of the structure so as to obtain the best beam pattern with highest gain possible. The optimized antenna produced a gain of 8.08dBi in azimuth plane at an elevation of 4 degrees from the ground plane. The antenna was fabricated and tested to verify the radiation pattern. It was found that there was a very close match between the designed and fabricated antenna.

Particle swarm optimization (PSO) is another optimization technique which received recent popularity for applications related to the design of antennas and microwave components. Reference [15] proposed a design of a non uniform circular antenna array using PSO. The PSO method was used to optimize the positions of elements arranged in a circular array. It was observed that PSO gave better results than GA optimization.

2.1 Circular Array Antenna Theory

Single antennas usually provide low directivity with a wide radiation pattern. Several antennas can be arranged in space and can be interconnected to produce a directional radiation pattern. Such configuration is referred to as an array antenna. Array antennas offer an efficient means for providing azimuth beam scan with limited elevation coverage. When the elements of the array are placed along a circular ring it is known as a circular array. Its applications are found in radio direction finding, air and space navigation, underground propagation, radar, sonar, and other systems including smart antennas [6].

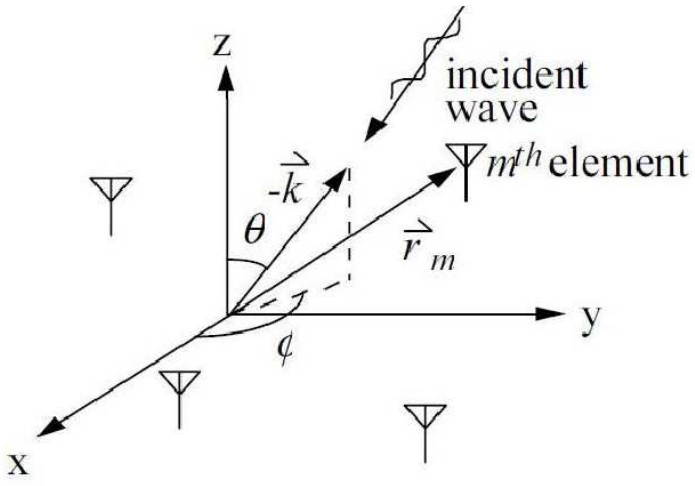

Figure 2.1: An arbitrary array antenna

2.1.1 Radiation pattern of a general array

An arbitrary array antenna in three dimensional space as shown in Fig. 2.1 is considered. It is assumed that the source of incident wave is a plane wave and is present in the far field of the array. The spherical coordinates of a vector from origin to the m^{th} element of the array is given by $\vec{r_m} = (\rho_m, \theta_m, \phi_m)$ and a unit vector in the

direction of the incident wave is given by $-\hat{k} = (1, \theta, \phi)$. The phase of the received plane wave at the m^{th} element is the phase constant $\beta = 2\pi/\lambda$ multiplied by the projection of the element position $\vec{r_m}$ onto the plane wave arrival vector $-\hat{k}$. This is given by $\vec{k} \bullet \vec{r_m}$ with the dot product taken in rectangular coordinates. In rectangular coordinates, $-\hat{k} = sin\theta cos\phi\hat{x} + sin\theta sin\phi\hat{y} + cos\theta\hat{z} = \hat{r}$ and $\vec{r_m} = \rho_m sin\theta_m cos\phi_m\hat{x} + \rho_m sin\theta_m sin\phi_m\hat{y} + \rho_m cos\theta_m\hat{z}$ and the relative phase of the incident wave at the m^{th} element is $\varsigma_m = -\vec{k} \bullet \vec{r_m} = \beta\rho_m(sin\theta cos\phi sin\theta_m + sin\theta sin\phi sin\theta_m sin\phi_m + cos\theta cos\phi_m)$ $= \beta(x_m sin\theta cos\phi + y_m sin\theta sin\phi + z_m cos\theta)$

2.1.2 Array factor

For an array of M elements, the array factor is given by

$$AF(\theta, \phi) = \sum_{m=1}^{M} I_m e^{j(\varsigma_m + \delta_m)}$$

where I_m is the magnitude and δ_m is the phase of the weighting of the m^{th} element. The normalized array factor is given by

$$f(\theta, \phi) = \frac{AF(\theta, \phi)}{max|AF(\theta, \phi)|}$$

2.1.3 Array pattern

If each element has a pattern $g_m(\theta, \phi)$, which may be different from other elements, the normalized array pattern is given by

$$F(\theta, \phi) = \frac{\sum_{m=1}^{M} I_m g_m(\theta, \phi) e^{j(\varsigma_m + \delta_m)}}{max(|\sum_{m=1}^{M} I_m g_m(\theta, \phi) e^{(j(\varsigma_m + \delta_m)}|)}$$

In the above equation, the element patterns must be represented such that the pattern maxima are equal to the element gains relative to a common reference.

2.2 Array Design

This work describes a planar circular array antenna. It consists of an array of 17 elements placed on a hollow cylindrical ground structure. Among the 17 elements 16 are distributed uniformly on the circumference of the 2 concentric rings and the other element is placed on the center of the ground structure.

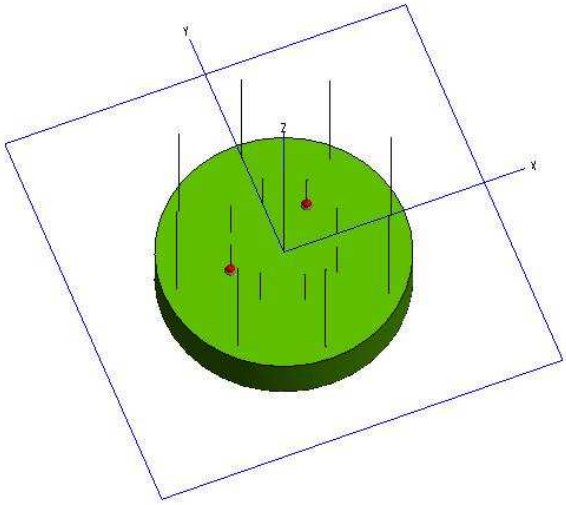

Figure 2.2: Geometry of the array antenna.

Fig. 2.2 shows the geometry of the antenna. Two driven elements shown with red ports in Fig. 2.2 are chosen such that they are placed 135 degrees apart on the inner ring. The elements placed diagonally opposite to the excited elements are grounded to act as reflectors. The elements behind the excited elements in the outer ring, the element at the center are also grounded and the remaining parasitic elements are removed from the system. So there are only 9 active elements which provide the desired directional beam in every case. The main beam of the radiation pattern is observed along the line bisecting the angle of the driven elements. The

driven elements are fed equally through a Wilkinson power splitter located beneath the cylindrical ground.

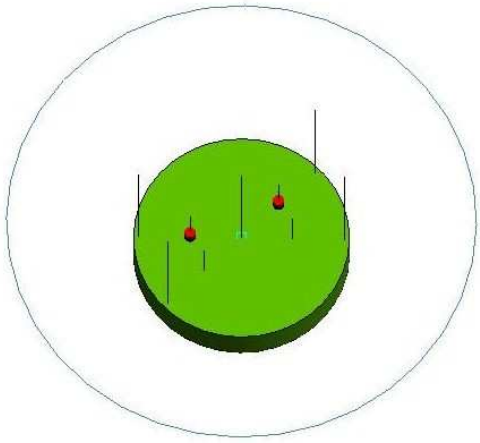

Figure 2.3: Geometry of the antenna with only essential elements.

Fig. 2.3 shows the geometry of the design with only the essential elements required in producing the desired beam pattern. The dimensions of the antenna structure are obtained by applying a particle swarm optimization technique with the help of FEKO simulation software. The dimensions and parameters for optimization are presented in detail in the next chapter.

Chapter 3

SIMULATION SOFTWARE: FEKO

FEKO is simulation software used for analyzing a wide range of electromagnetic problems involving objects of arbitrary shapes. FEKO is an abbreviation derived from the German phrase *FEldberechnung bei Korpern mit beliebiger Oberflache* (Field computations involving bodies of arbitrary shape). Some of its applications include EMC analysis, antenna design, microstrip antennas and circuits, dielectric media, scattering analysis [11]. It could be installed on MS Windows or Linux based PC's or work stations. The time required for FEKO to simulate a design is very low compared to other electromagnetic softwares like HFSS which takes several hours for a single basic simulation.

FEKO is based on the method of moments (MoM) technique. In this method the electric surface currents on the conducting structures are calculated to ascertain the electromagnetic fields. Multilevel Fast Multipole Method (MLFMM), the Finite Element Method (FEM), Uniform Theory of Defraction (UTD), Geometrical Optics (GO) and Physical Optics (PO) are also used when solving electrically large problems and inhomogeneous dielectric bodies of arbitrary shape. The PO approximation or the UTD are hybridized with the MoM in order to be utilized by FEKO. Because of this hybridization technique, any critical region of a structure can be evaluated using the MoM while the remaining regions, that may be larger, flat or curved, can be analyzed using the PO approximation or UTD. Fig. 3.1, shows the diverse applications of FEKO software and various techniques used depending on the electrical size of the structure.

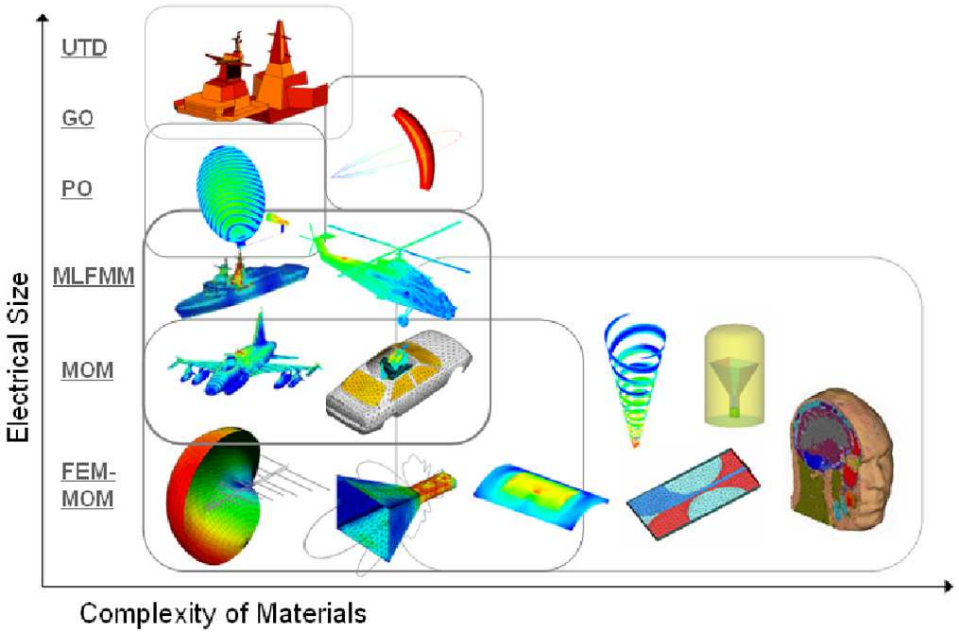

Figure 3.1: Diverse applications of FEKO software(Figure obtained [11])

3.1 Method of Moments

The MoM is a full wave solution of Maxwell's integral equations in the frequency domain. MoM is a "source method" which means that only the geometric structure of the antenna is discretized, not free space. It is used for modeling open boundary radiating structures where no 3D space discretization is required.

The conductors in the antenna structure can be broken into "segments", and the current flowing through each of these segments can be determined. The value obtained by multiplying the current with the vector describing the little segment (length and orientation) is termed as "Moment" [18].

A set of "basis functions" may be assumed into which the current distributions are decomposed. These basis functions could be a rectangular approximation to the Dirac delta function. Because the widths of the rectangular sections are non-zero, only a finite number of them are enough to cover the antenna wire structure. Another

type of basis function is triangular in shape. They give a smoother approximation to the current distribution. The current distribution is piecewise-linear between the matching points. In general, the "n^{th} moment" is obtained by integrating the product of the Green's function with the n^{th} basis function [18].

The "method of moments" starts from deriving the currents on each segment, or the strength of each moment, by using a coupling Green's function. The Green's function includes electrostatic coupling between the moments which helps in calculating the buildup charge at all the points if the spatial change of the currents is known accurately [18].

A Green's function is a kind of 3-dimensional version of the impulse response function familiar in linear electronic circuit analysis. One sets up a structure for the space under consideration, specifying where the excitations can be and what the boundary conditions are. One then excites the structure with a single little region of excitation, with all the other possible excitations set to zero. The Green's function is the response of all the other regions in the problem to this excitation. Since the system is assumed linear, the principle of superposition applies and the total response to an arbitrary set of excitations can be obtained for the problem by direct summation or integration over all the excitations. The far field can be computed from moments defined at each segment of the antenna [18].

3.2 FEKO Suite components

FEKO consists of the following major user interfaced units which aid from designing the antenna to obtaining the radiation patterns: CADFEKO, EDITFEKO, POSTFEKO [11].

CADFEKO is a graphical environment in which the geometry and mesh can be created. We can specify the solution settings and calculation requirements here. From CADFEKO other modules of FEKO can also be accessed. It displays three dimensional antenna geometry, which allows the user to view the antenna structure from all angles and verify the geometry. It also displays other information, such as meshing and three-dimensional field patterns.

EDITFEKO is used to construct advanced models both in terms of the geometry and solution requirements with the help of a high level scripting language.

POSTFEKO displays polar and linear plots of the S-parameters, 3D far fields, 2D and 3D near fields.

3.3 Optimization

Optimization is a procedure for choosing the best possible solution for a given problem among the available alternatives. This could be achieved by changing the parameters which could affect the desired result or response. In a geometric model the parameters are mostly dependent on the dimensions or material properties or the excitation of the structure. Optimization is based on various aspects like

- Method to be used, which defines the optimization technique that should be used for each particular type of problem.
- Parameters, which define the range in which the search is conducted.
- Goals, which define the final desired output of the search [11]

3.3.1 OPTFEKO

The optimization process in FEKO is carried out by the OPTFEKO unit. Various optimization methods like Genetic Algorithm (GA), Particle Swarm Optimization,

Simplex Nelder- Mead algorithm and Grid search could be performed in FEKO. After running various simulations to identify the optimization method suitable for the antenna design in this work, it was observed that the particle swarm optimization method offered the best configuration for the antenna.

3.3.2 Particle Swarm Optimization

The particle swarm optimization (PSO) algorithm was first introduced by James Kennedy and Russell Eberhart in 1995. It is less cumbersome compared to algorithms like genetic algorithm (GA) as it could be implemented with minimal mathematical processing. It has evolved as a powerful optimization tool in solving mathematical functions as well as electromagnetic problems. Therefore in this work PSO algorithm is used to optimize the dimensions of the design so as to maximize gain of the antenna in desired direction.

The algorithm could be easily explained by considering an analogy to a swarm of bees in search of flowers in a garden. The objective of bees is to find a location in the garden where maximum number of flowers are concentrated. An assumption is made that the bees do not have prior knowledge of the garden. The bees fly randomly in different directions with different velocities. When a bee finds a location with maximum flowers, i.e. its personal best location, it remembers the location and informs the whole swarm about the location. In this way, each bee has the knowledge about the best location, i.e. global best location found so far. Based on nostalgia or social influence the bee continues its navigation through locations between the personal best location and global best location. This is a continuous process and a bee can be in any location, even the exact location where the other bees have been.

Along the way, a bee might find a new location with higher concentration than before. It would then be attracted to this new location as well as the location of

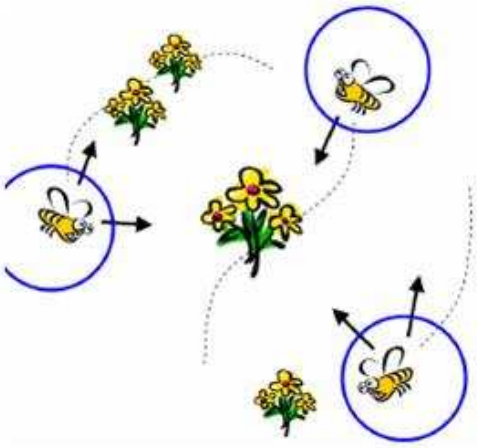

Figure 3.2: Particle Swarm Optimization as modeled by a swarm of bees searching for flowers (Figure obtained from [13])

the most flowers found by any bee in the whole swarm. In this way the bees explore the whole garden and eventually find the location with the highest concentration of flowers.

For carrying out a particle swarm optimization in FEKO, the default swarm size is set to 20 and the number of iterations to 50, resulting in 1000 solver runs. The maximum number of solver runs, (C), could also be specified by the user by maintaining a condition that when the number of solver runs is converted into a population size (A) and number of iterations (B), $A * B \leq C$. A is selected as a function of the number of parameters (Np), and B $\geq$ 5 must always be satisfied.

3.4 Simulation of the antenna model in FEKO

The antenna design is created in the CADFEKO component of FEKO which supports the creation and setup of FEKO models. Fig. 3.3 shows the CADFEKO display containing the antenna design and various tool bars. The tool bar at the top is used to make modifications in the display of the model. The tool bar at the left is

used for geometry creation, modification, transform, solutions, network creation and optimization.

First of all the unit for the models dimensions is selected(meters) and then the variables are assigned values in terms of wavelength. These variables define the various dimensions of the design model. Following is the list of variables used:

- hc= 0.2500λ (Height of the cylindrical ground plane)
- rc= 0.6000λ (Radius of the cylindrical ground plane)
- hi= 0.2500λ (Height of elements on inner circle)
- ho= 0.2750λ (Height of elements on outer circle)
- horg= 0.2667λ (Height of element at origin)
- ri= 0.2667λ (Radius of inner circle)
- ro= 0.5334λ (Radius of outer circle)

Next the antenna design is created by choosing the required shapes from the geometry tool bar. A hollow cylinder with all the elements mounted on it is created. The elements I, II with ports marked at the bottom as shown in Fig. 3.3 are chosen for excitation and 1V is applied to them. The frequency of operation of the antenna is designated as 2GHZ.

The far field request is created named 'H-Plane' with parameters set at

- $theta = 85^\circ$ to 90°
- $phi = 0^\circ$ to 360°

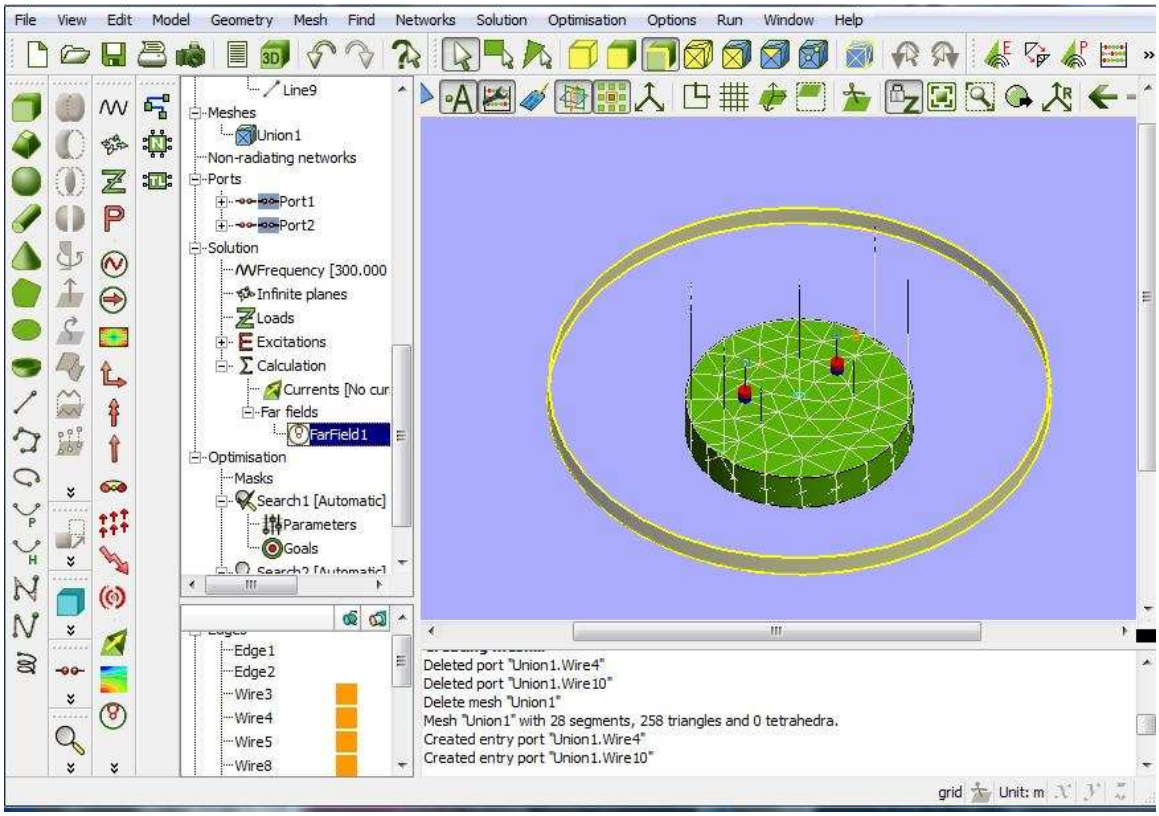

Figure 3.3: CADFEKO view showing the meshing and far field parameters of the antenna

The model is then meshed choosing edge length = 0.2λ, Segment length = 0.2λ, Wire radius = 0.01λ.

A Particle Swarm Method (PSO) optimization search is included. The parameters shown in Fig.3.4 have been defined for optimization.

The optimization goal is selected so as to maximize the gain of the antenna design. The simulation is run and 1000 optimization solvers are completed before the final optimized dimensions are obtained. The optimization was carried out in several steps. In the first step the dimensions of the cylinder (i.e. the height and the radius of the cylinder) was optimized. In the second step the lengths of the wire antenna elements on the ground plane were optimized.

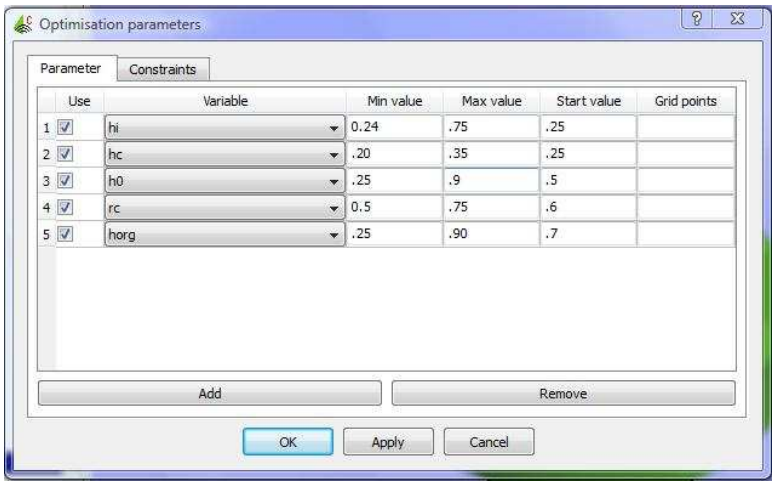

Figure 3.4: Parameters for Particle swarm optimization

3.5 Optimal Geometry

After optimization was conducted a new set of optimized values for the dimensions were obtained which could maximize the gain of the antenna. Following is the list of optimized dimensions of the design

- hc= 0.2000 λ (Height of the cylindrical ground plane)
- rc= 0.5600 λ (Radius of the cylindrical ground plane)
- hi= 0.2545 λ (Height of elements on inner circle)
- ho= 0.7990 λ (Height of elements on outer circle)
- horg= 0.7970 λ (Height of element at origin)
- ri= 0.2667 λ (Radius of inner circle)
- ro= 0.5334 λ (Radius of outer circle)

3.6 Results

Fig. 3.5 presents the antenna configuration with all the elements shown i.e. the configuration that is practically used.

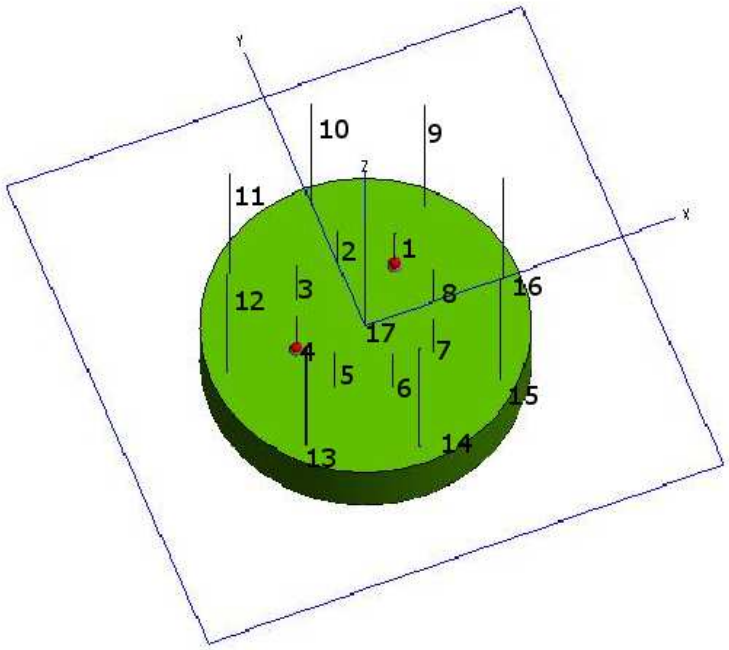

Figure 3.5: Geometry of the complete antenna array

Fig. 3.6[a] shows the radiation pattern of the antenna when elements (shown in Fig. 3.5) 1 and 4 are excited and the elements 5, 8, 9, 12, 13, 16, 17 are grounded and other elements are removed from the system (i.e, they are open circuited).Fig 3.6[b] is obtained when the 2 and 5 elements are excited and the elements 1, 9, 6, 10, 13, 14, 17 are grounded and other elements are removed from the system. Thus the pattern rotates in the azimuth plane with change in the antenna coniguration.

A switching circuit is placed underneath the antenna to select and excite the required elements in order to steer the beam in the desired direction.

The following figures show the simulated radiation pattern of the antenna. The gain of the pattern is 9.8dB and the beamwidth is 55 degrees. The angle of elevation of the beam was measured as 5 degrees from the horizontal plane.

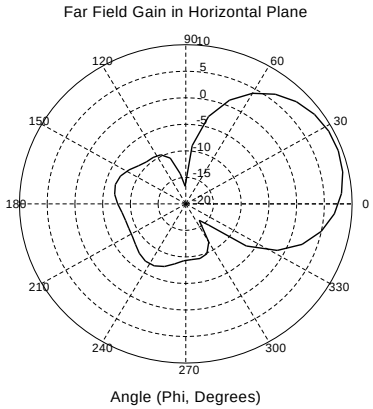

[a]

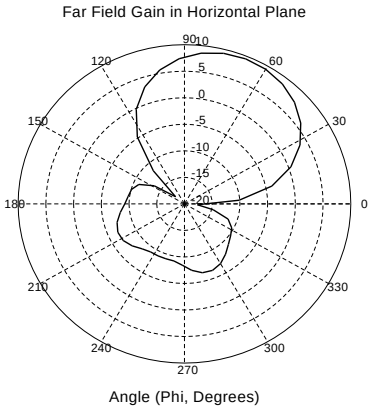

[b]

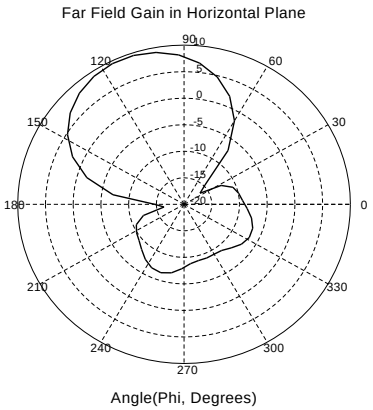

[c]

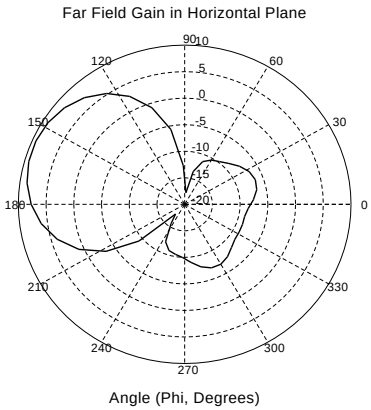

[d]

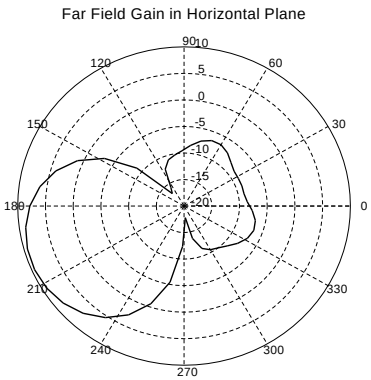

[e]

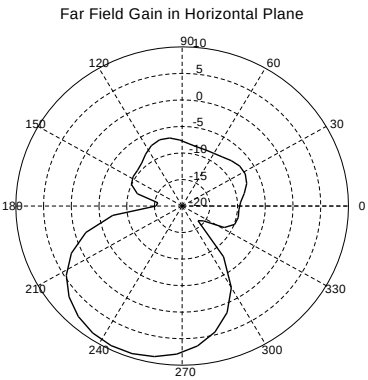

[f]

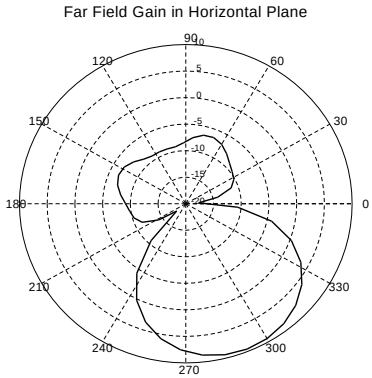

[g]

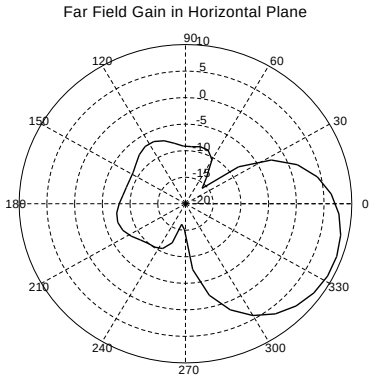

[h]

Figure 3.6: Radiation patterns for the antenna

3.6.1 Observations

It is observed that the elements in the outer circular ring acted as reflectors and the elements in the inner circle directed the beam such that the main beam is concentrated in the direction of diagonal between the excited elements. The element present at the center of ground plate helped in reducing the side lobe value of the

radiation pattern. Simulations should be carried out by changing the positions of the elements and the number of elements being used in the radiation mechanism to obtain better radiation pattern with a higher gain.

Fig. 3.7 shows the radiation pattern, when the 17 element antenna configuration shown in Fig. 3.5 system is considered.

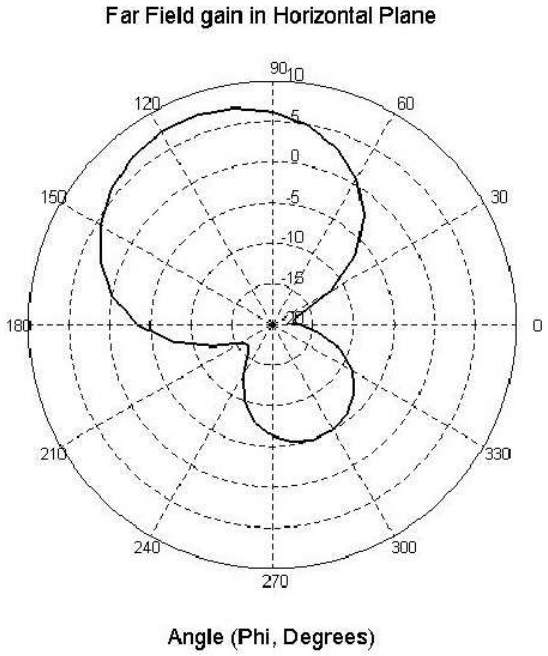

Figure 3.7: Radiation pattern of antenna

The gain of the pattern is 8dB and the beamwidth is 58 degrees at 5 degrees elevation from the horizontal plane. Fig. 3.8 compares the radiation pattern of the 9 element system with the 17 element system. It is observed that the unused elements contributed to the interaction and coupling which reduced the gain of the system. It is also observed that the amount of side lobe for the 17 element system is less compared to the 9 element system.

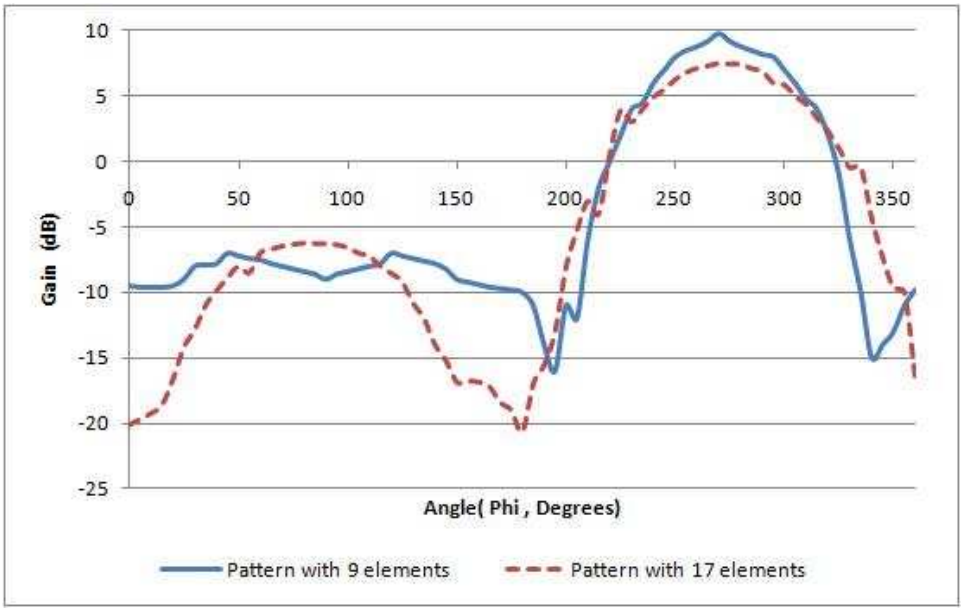

Figure 3.8: Comparison of radiation patterns for different antenna configurations

3.7 Antenna design with improved gain

Though the previous design has been sent for fabrication further simulations have been carried out to design an antenna with better gain characteristics. In these optimizations the limits of the design parameters were further extended and the radius of the circular rings on which the elements lie has also been optimized. It was observed that by increasing the diameter of the cylindrical ground plane the gain of the structure improved notably. In the new configuration elements were added in both the inner and outer circles in the positions behind the excited elements such that there are 4 elements 45 degrees apart from each other behind the excited elements in both the concentric circular rings. Fig. 3.9 shows the configuration of the new antenna design. The elements displayed with red and yellow ports are the excited elements.

Following is the list of optimized dimensions of the design

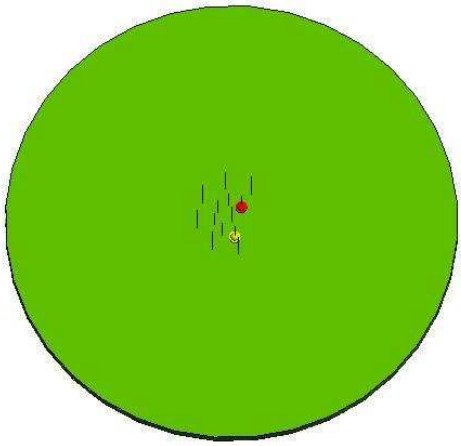

Figure 3.9: Geometry of the new antenna design

- $hc = 0.1775\lambda$ (Height of the cylindrical ground plane)
- $rc = 3.5000\lambda$ (Radius of the cylindrical ground plane)
- $hi = 0.5974\lambda$ (Height of elements on inner circle)
- $ho = 0.8933\lambda$ (Height of elements on outer circle)
- $horg = 0.7844\lambda$ (Height of element at origin)
- $ri = 0.2667\lambda$ (Radius of inner circle)
- $ro = 0.5334\lambda$ (Radius of outer circle)

3.7.1 Radiation Patterns

A gain of 12dB was observed with this configuration at 10 degrees elevation from the horizontal plane. The following figures show the radiation patterns of the design.

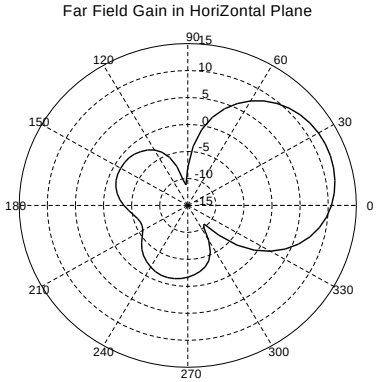

[a]

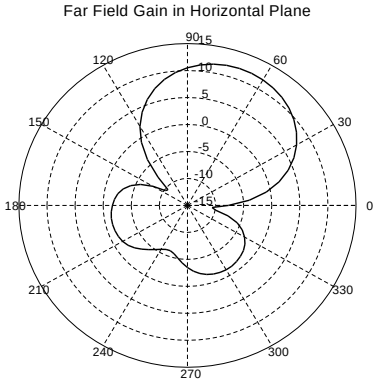

[b]

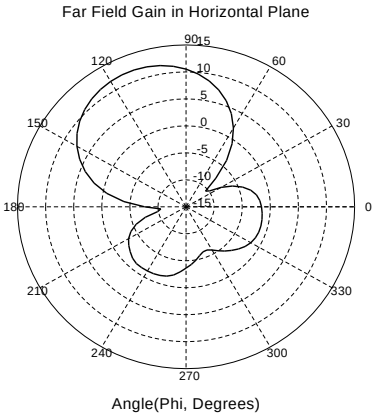

[c]

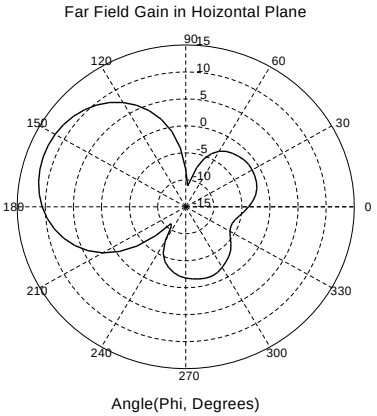

[d]

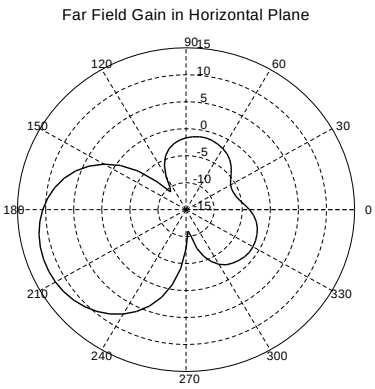

[e]

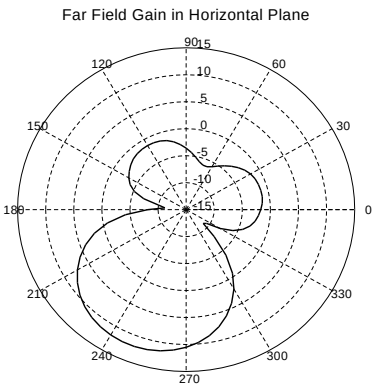

[f]

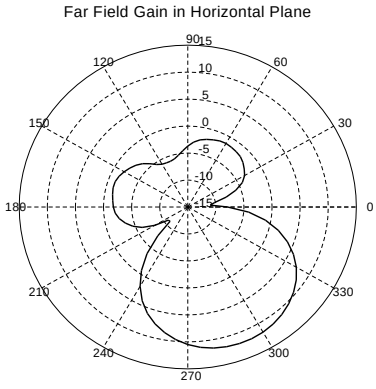

[g]

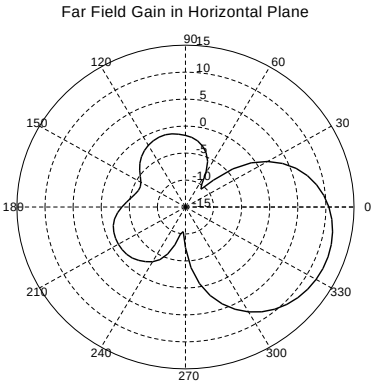

[h]

Figure 3.10: Radiation patterns for the new antenna

3.7.2 Observations

Various simulations have been performed to examine the effect of every element in the array on the radiation pattern. It was found that the presence of an element at the center of the ground plate reduced the amount of side lobe in the radiation

pattern. The elements in the outer circular ring acted as reflectors and the elements in the inner circle directed the beam such that the main beam is concentrated in the direction of diagonal between the excited elements. By adding the other elements in the circle behind the excited elements the pattern became stronger and achieved a higher gain. Hence these elements increased the directivity of the pattern. It was also observed that by increasing the radius of ground plate from 0.6λ to 2.5λ the gain of the pattern improved drastically. But when the radius of ground plane was further increased to 3.5λ the improvement in the gain of the pattern was very small only about 0.5dB. Therefore these changes were optimized following the particle swarm optimization to obtain the best dimensions for the antenna structure which could increase the gain. Though the new antenna dimensions made it bulkier it has greatly improved the gain of the system and decreased the angle of elevation of the pattern.

But with the increase in the radius of the ground plane, the angle of elevation of the pattern at which high gains were obtained reached about 10 degrees above the horizontal plane.

Chapter 4

Fabrication of the Antenna

For experimental validation, the antenna design acquired from the first optimization is fabricated. The antenna was fabricated to operate at 2 GHz frequency. The antenna was fabricated in Auburn University's Electrical Engineering work shop. Copper sheets were used to fabricate the cylindrical ground and copper rods of standard diameter very close to that of the optimized value were used for the elements. All the elements excluding the ones which are excited are screwed to the ground plate so that they could be removed if required. The two excited elements are connected to the power supply through a power splitter designed to distribute the power equally between the two excited elements. The complete version of the antenna is shown in Figures 4.1, 4.2

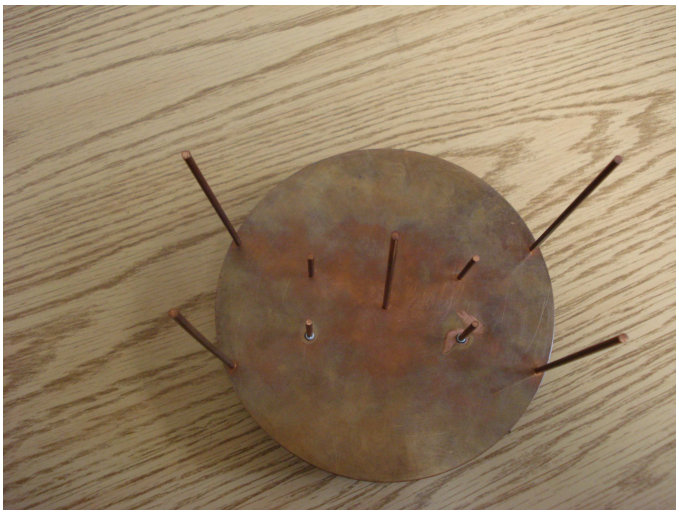

Figure 4.1: Top view of the fabricated antenna

Dimensions of the fabricated antenna are as follows:

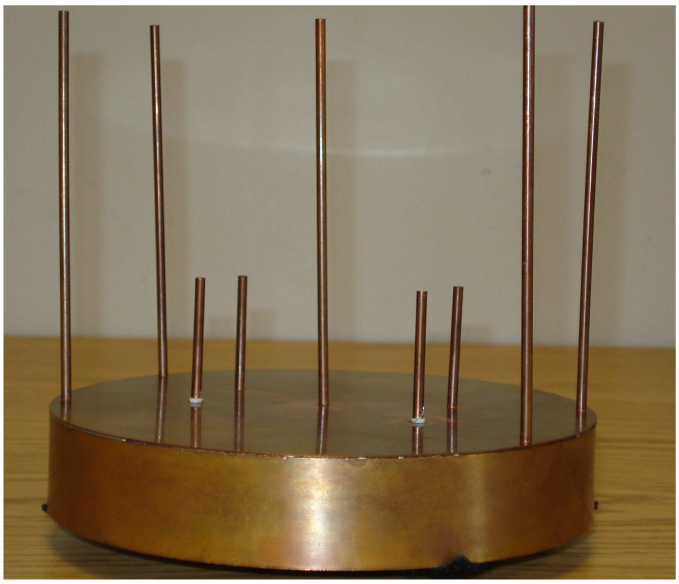

Figure 4.2: Side view of fabricated antenna

- hc= 1.1811 inches (Height of the cylindrical ground plane)
- rc =3.3070 inches (Radius of the cylindrical ground plane)
- hi =1.5029 inches (Height of elements on inner circle)
- ho = 4.7238 inches (Height of elements on outer circle)
- horg =4.7096 inches (Height of element at origin)
- ri = 1.5750 inches (Radius of inner circle)
- ro = 3.1500 inches (Radius of outer circle)
- rr = 0.0625 inches (Radius of antenna elements)

4.1 Feed Network for Antenna Array

For an array antenna, the feed network is used to regulate the amplitude and phase requirements of the radiating elements. Thus designing and implementing the feed network is an important part of antenna design. For the present design two elements are given voltage excitation which requires a power splitter which can distribute the power equally and in-phase between the two ports. Among the various power splitter circuits, a Wilkinson power divider is selected as it is lossless when the output ports are matched. By definition, it is a -3dB three port power divider device that divides power equally in magnitude and phase. Fig. 4.3 shows the block diagram of a power divider.

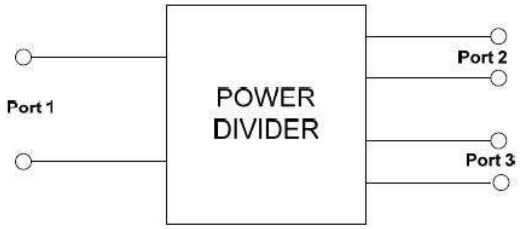

Figure 4.3: Block Diagram of power divider

Quarter wave transformers are used to match the split ports to the common port. Since a lossless reciprocal three port network cannot have all ports simultaneously matched, Wilkinson introduced a resistor for the purpose of matching. Apart from matching, the resistor also improves the isolation between the output ports. Fig. 4.4 shows the equivalent circuit and the microstrip implementation of a Wilkinson two-way power divider. The impedances required for the quarter wave transformer and the isolating resistor are also shown in this figure.

The dimensions of the design are as follows: $Z_1 = 50\Omega$, $Z_2 = 70.7\Omega$ and $R = 100\Omega$. The length of Z_2 elements for copper substrate is quarter of a guide wavelength

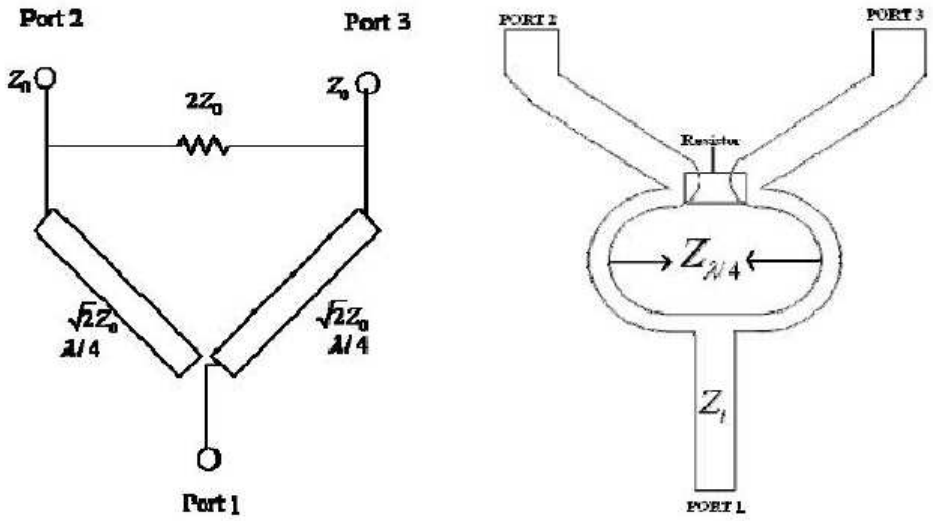

Figure 4.4: Wilkinson power divider and it equivalent microstrip line implementation

which equals to 3.75cms for a frequency of 2 GHz. Here the input port, port1, of the wilkinson circuit is terminated in 50Ω, and the output ports 2 and 3 are measured by ports 1 and 2 of the VNA. S_{22} is the reflection looking into port 2 and S_{32} is the signal coupled from port2 to port3. Hence S_{23} is a measure of isolation. The individual response of the power dividers are presented below. The transmission parameters (S_{21} and S_{31}) observed from Fig.4.5 shows they are very close to -3dB. It is of note that the performance of the divider is more acceptable at 1.8 GHz rather than 2 GHz.

It is evident from the Fig. 4.6 that the reflection parameters (S_{22} and S_{33}) are below - 20dB at 2GHz. The isolation parameters (S_{32} and S_{23}) shown in Fig.4.7 are less than -20dB.

Following figures show the fabricated Wilkinson power splitter being connected to the ports of the antenna.

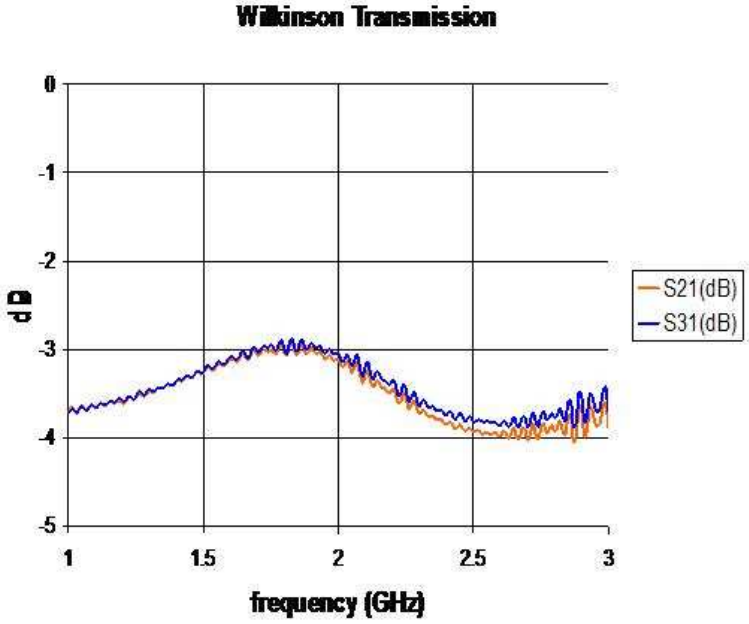

Figure 4.5: The transmission parameters of Wilkinson power splitter

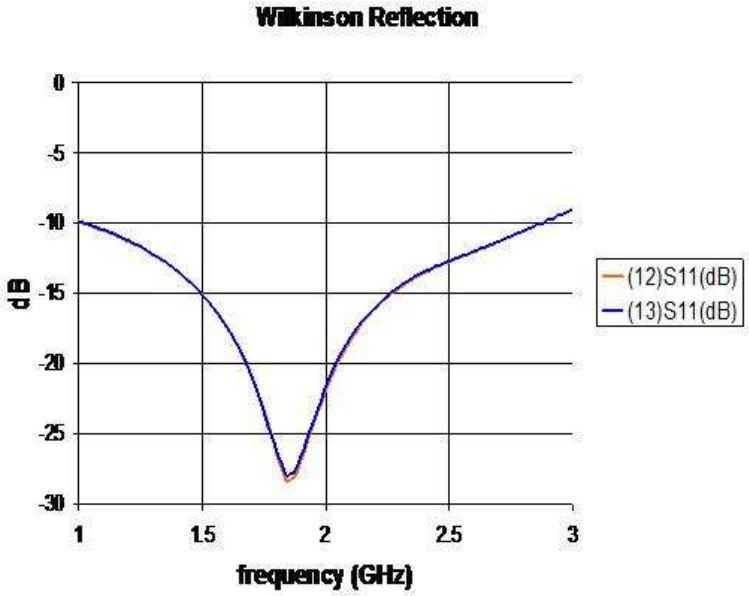

Figure 4.6: Reflection parameters of Wilkinson power splitter

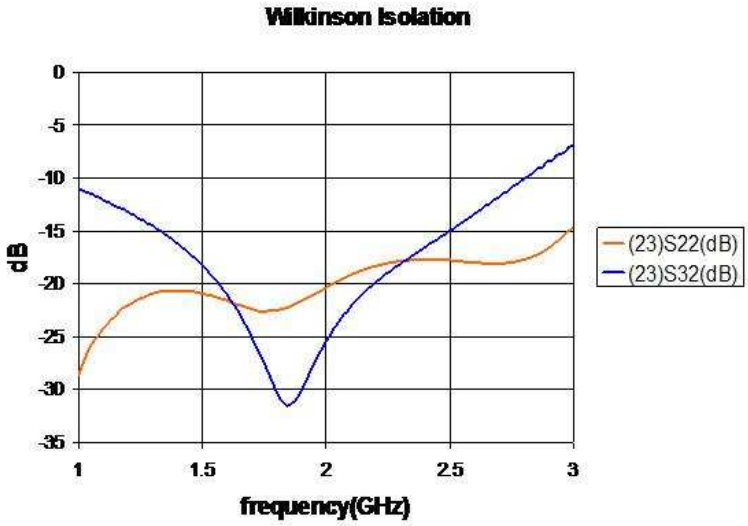

Figure 4.7: Isolation parameters of Wilkinson power splitter

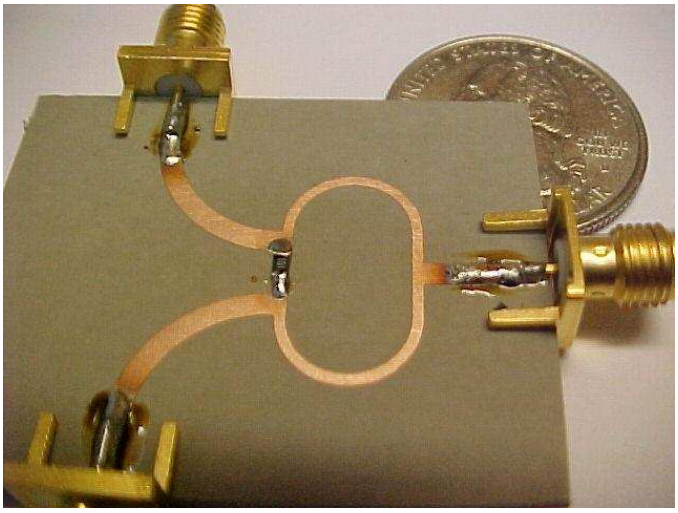

Figure 4.8: Fabricated Wilkinson Power Divider

Figure 4.9: Power Splitter connected to the ports of the antenna

Chapter 5

Experimental Verification

The radiation pattern measurements have been carried out in the anechoic chamber of Antenna Laboratory at Auburn University. Indoor anechoic chambers have been developed to provide a controlled environment for testing the performance of the antennas. These can overcome problems related to outdoor testing. An anechoic chamber is an enclosure lined completely with radiation absorbent material (RAM) to simulate a quiet, free-space like environment for testing the radiation patterns of antennas. Only the antenna to be tested and equipment required to perform the measurements are allowed inside the anechoic chamber. Far field measurements can be carried out in this chamber to measure the antenna characteristics like gain, beamwidth, and side lobe level. The RAM is responsible for absorbing the incident RF radiation from all possible directions. They generally comprise an array of pyramid shaped pieces made up of rubberized foam material impregnated with controlled mixtures of carbon and iron. Fig. 5.1 shows an RF anechoic chamber.

5.1 Measuring the Resonant Frequency and input impedance

The network analyzer was first calibrated before proceeding with the measurements. The resonance frequency and the input impedance measurement values of the fabricated Planar Circular array antenna were obtained as follows.

- Resonant Frequency= 2GHz
- Input impedance = 25+j12 Ω

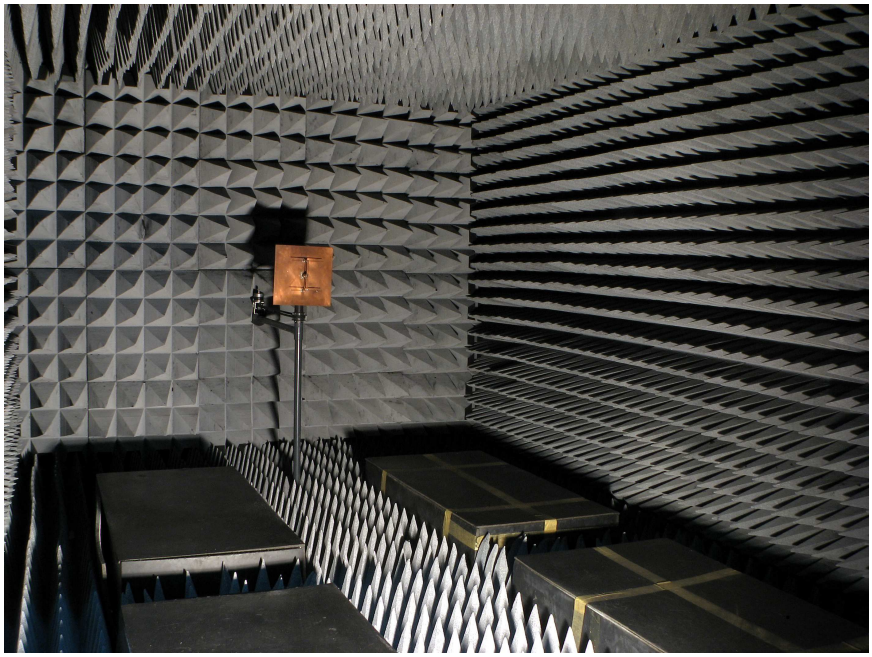

Figure 5.1: An RF anechoic chamber

The impedance of an antenna is the impedance at the antenna terminals with no load attached, impedance may be defined as the ratio of the voltage to current at the antenna terminals. Maximum power transfer can be achieved when the impedance of the antenna is matched to that of the load. If there is an impedance mismatch then part (or all) of the power is reflected rather than radiated. The amount of the wave reflected depends on how bad the mismatch is.

Voltage Standing Wave Ratio (VSWR) is a measure of impedance mismatch between the transmission line and its load. The higher the VSWR, the greater is the mismatch.

- The VSWR ratio was measured as 1.8±0.6 at 2GHz frequency as shown in the Fig. 5.2

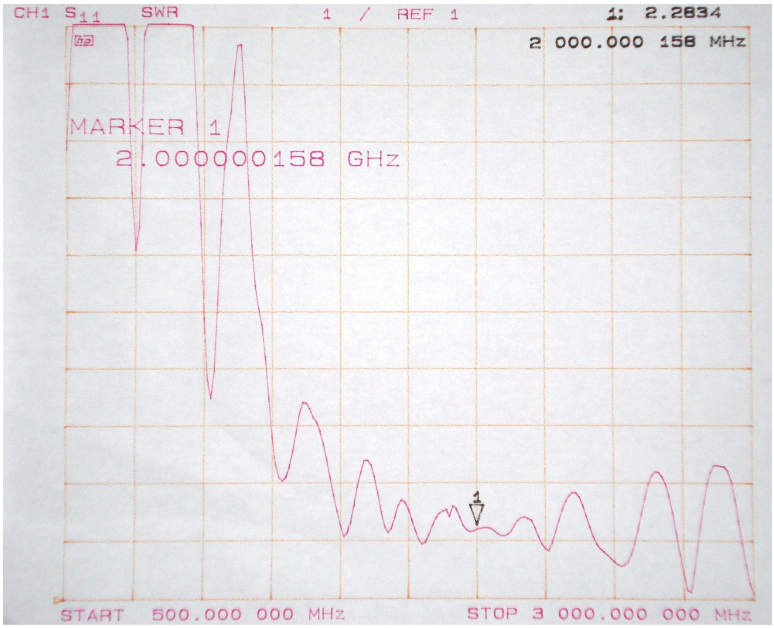

Figure 5.2: SWR measurement of the antenna

5.2 Measuring the gain of the antenna

In the anechoic chamber there are two platforms for placing the source antenna and test antenna. The platforms were separated with a distance of about 136 inches. A Scientific Atlanta's standard gain horn antenna SGH 1.7 was used as source antenna. The antenna under test (the fabricated Planar Circular Array antenna) was placed at the receiving end on the tripod stand of the Desktop Antenna Measurement System (DAMS). Fig. 5.3 shows the (DAMS) tripod stand.

The DAMS is designed to aid the testing of small antennas. It can calculate the path loss and gain of the antenna. The setup comprises of a tripod stand to place the test antenna, platform controller which connects the computer to the tripod stand and controls the movement of the platform. The platform on the tripod stand can rotate 360 degrees in the horizontal direction and from +45 to -45 degrees in the vertical direction.

Figure 5.3: DAMS tripod stand (Figure obtained from [12])

As the antenna had an SMA connector at the bottom it could not stay flat when placed on the tripod. To fix this problem a small hollow rectangular wooden block was fixed on the stand with the help of foam tapes and the antenna was fixed on the block as shown in Fig. 5.4. Before the measurements were made the source and test antenna were properly aligned with the help of a laser aligner. A supply power of 25dBm was provided to the horn antenna through the analyzer. Then the DAMS software was activated so that the platform of the tripod stand rotates 360 degrees horizontally. The far field radiation pattern measurements at each position were recorded. The measurements were taken with an interval of 10 degrees.

Fig. 5.5 shows the step wise procedure followed in performing the radiation pattern measurements. The measurement setup was calibrated by selecting the range about which the platform moves in horizontal and vertical direction. In this case the platform is subjected to rotate 360 degrees in the horizontal direction. A horizontal scan was then performed and the data is saved to plot the radiation pattern using DAMS software.

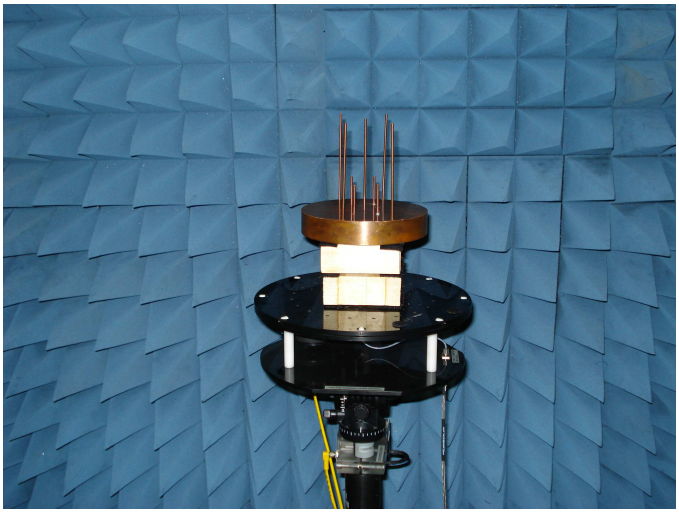

Figure 5.4: Antenna placed on wooden block for support

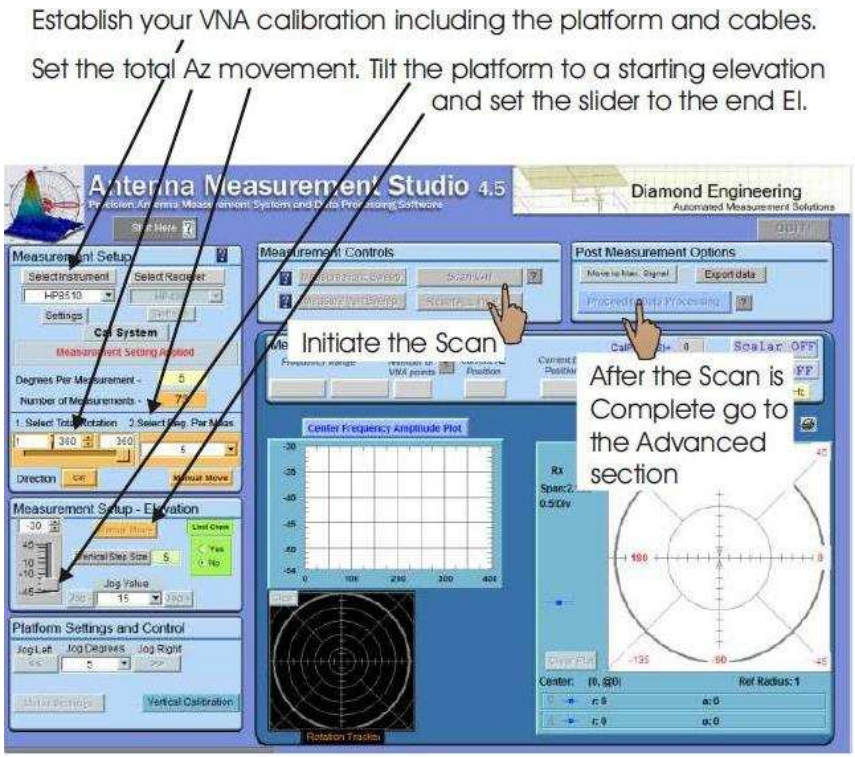

Figure 5.5: Initializing a measurement in DAMS (Figure obtained from [12])

5.3 Results

Fig. 5.6 shows the radiation pattern of the antenna in the horizontal plane. The gain of the antenna was measured as 9.3dB. *Beamwidth* is the directiveness of

a directional antenna, defined as the angle between two half-power or -3 dB points on either side of the main lobe of radiation. Our antenna had a measured BW of 60 degrees.

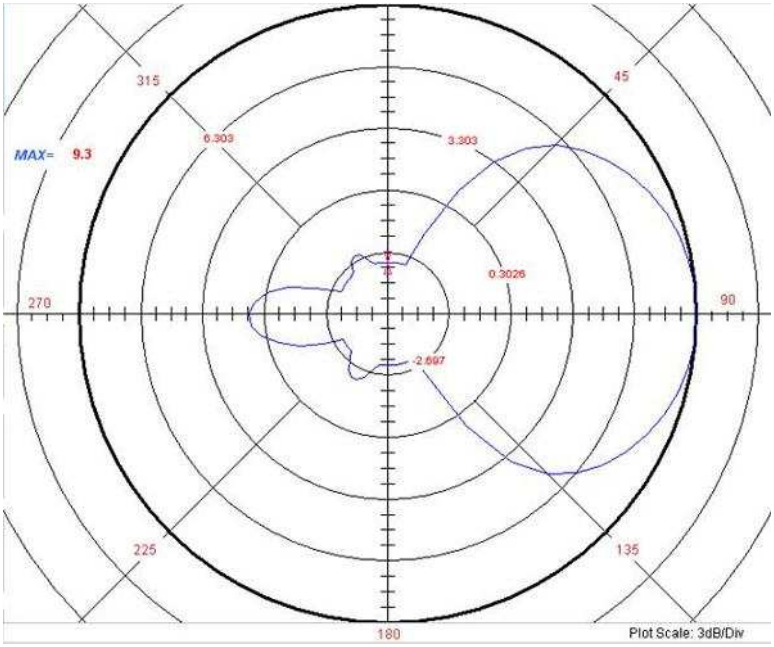

Figure 5.6: Radiation pattern in Horizontal plane

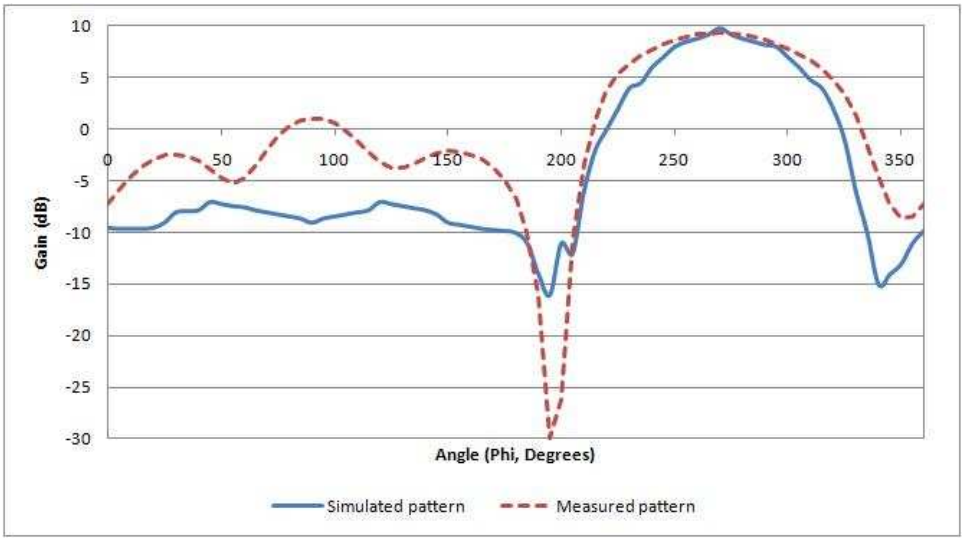

Figure 5.7: The simulated and measured radiation patterns of antenna

Fig. 5.7 compares the radiation pattern of both simulated and experimental radiation pattern. It is observed that the side lobe value of fabricated antenna is more than that of the designed antenna. The difference in the gain of the fabricated antenna when compared to the simulation result may be due to the impedance mismatch at the inport port of the antenna. An impedance matching circuit can be designed to overcome this problem.

Chapter 6

Conclusion

In this work, a dual excited planar circular array antenna implementing electronic beam steering over 360 degrees azimuth useful for direction agile applications is presented. A PSO algorithm was applied to optimize the antenna's structure so as to provide maximum gain in the horizontal plane in the direction of a diagonal between the two excited elements. This antenna has been successfully developed after running numerous simulations using FEKO software package to get the best combination of parameters for overall performance. This was followed by the fabrication and testing phases. From the FEKO simulations, a gain of 9.8dB was obtained at 5 degrees elevation from the azimuth plane with a beam width of 55 degrees.

The experimental validation presented in this work is restricted to the electromagnetic behavior of the antenna, and ignores the driving circuit. The experimental verification was carried out using a scale model at 2 GHz. The impedance measurements were carried out using the network analyzer and the radiation pattern measurements were conducted in the anechoic chamber of the Antenna Laboratory at Auburn University. The results were in good agreement with the simulated results, even though there were minor differences. The gain of the fabricated antenna was 9.3dB, the input impedance was measured to be 20+j12 Ω and the beam width measured as 60 degrees.

Another improved design was simulated and its results were presented. A gain of 12 dB was achieved at an elevation of 10 degrees from the horizontal.The elements that were theoretically considered to be open were removed from the system during the

experiment. Although, theoretically it is possible to open these elements and eliminate them from radiation mechanism, practically the unused elements do contribute for the interaction and coupling which may deteriorate or alter the pattern.

Hence the future work in developing the array antenna would constitute a design in which all the elements of the system are used and to optimize the antenna structure to reduce the angle of elevation of the main beam and to improve the radiation pattern such that the value of side lobes is reduced much further.

Bibliography

[1] "How Mobile Phone Networks Work" online at
http://www.ofcom.org.uk/mobilework.htm

[2] Sibille, C. Roblin, and G. Poncelet, "Circular switched monopole arrays for beam steering wireless communications," Electron. Lett., vol. 33, no. 7, pp. 551-552, Mar. 1997.

[3] "Cellular telephone basics" online at
http://www.privateline.com/Cellbasics/Cellbasics14.html

[4] The Bell Labs Technical Journal, pp 15-41, January 1997,.

[5] R. Schlub, J. Lu, and T. Ohira, "Seven-Element ground skirt monopole ESPAR antenna design from a genetic algorithm and the finite element method," Trans. IEEE Antennas Propag., vol. 51, no. 11, pp. 3033-3039, Nov. 2003.

[6] C. A. Balanis, Antenna Theory Analysis and Design, 2nd ed. NewYork: Wiley, 1997.

[7] W.L. Stutzman and G.A. Thiele, Antenna Theory and Design, John Wiley and Sons, 1998

[8] S. K. Sharma and L. Shafai, "Beam Focusing Properties of Circular Monopole Array Antenna on a Finite Ground Plane," Trans. IEEE Antennas Propag., vol. 53, no. 10, pp. 3406-3409, Oct. 2005.

[9] H. Scott and V. F. Fusco, "360 Electronically Controlled Beam Scan Array," Trans. IEEE Antennas Propag., vol. 52, no. 1, pp. 333-335, Jan. 2004.

[10] S. C. Panagiotou, T. D. Dimousios, S. A. Mitilineos, and C. N. Capsalis, "Broadband Switched Parasitic Arrays for Portable DVB-T Receiver Applications in the VHF UHF Bands," Trans. IEEE Antennas and Propag., vol. 50, no. 5, October 2008.

[11] FEKO Suite 5.4,User's Manual

[12] Diamond Engineering's Desktop Antenna Measurement System (DAMS) user manual and setup guide.

[13] J. ROBINSON, Y. RAHMAT SAMII, " Particle swarm optimization in electromagnetic," Trans. IEEE Antennas Propag., vol. 52, no. 2, pp.397-407, Feb. 2004.

[14] K. R. Mahmoud, M. I. Eladawy, Rajeev Bansal, S. H. Zainud-Deen, S. M. M. Ibrahem," Analysis of Uniform Circular Arrays for Adaptive Beamforming Applications Using Particle Swarm Optimization Algorithm," International Journal of RF and Microwave Computer-Aided Engineering, vol. 18 , no. 1, pp. 42-52, January 2008.

[15] M. M. Khodier, Nihad Dib,"Design of Non Uniform Circular Antenna Arrays Using Particle Swarm Optimization," Journal of ELECTRICAL ENGINEERING, vol. 59, no.4, pp216-220, 2008.

[16] K.L. Du, "Pattern analysis of uniform circular array," Trans. IEEE Antennas Propag., vol. 52, pp. 11251129, (2004).

[17] R. T. Compton, Jr., "A Method of Choosing Element Patterns in an Adaptive Array," Trans. IEEE Antennas Propag., vol. 30, no. 3, pp. 489-493, May 1982.

[18] "Method of Moments for Antenna Calculations" online at http://personal.ee.surrey.ac.uk/Personal/D.Jefferies/mmethod.html

[19] R. Vaughan, "Switched Parasitic Elements for Antenna Diversity," Trans. IEEE Antennas Propag., vol. 47, no. 2, pp. 399-405, February 1999.

[20] P. Ioannides, and C. A. Balanis,"Uniform Circular and Rectangular Arrays for Adaptive Beamforming Applications ," Trans. IEEE Antennas and Wireless Propog., vol. 4, pp. 351-354, 2005.

[21] D. V. Thiel and S. Smith, Switched Parasitic Antennas for Cellular Communications. Norwood, MA: Artech House, ch. 4, 2002.

[22] R. F. Harrington, "Reactively controlled directive arrays," Trans. IEEE Antennas Propaga., vol. 26, pp. 390395, May 1978.

[23] E.K. Walton and J.D. Young, "The Ohio state university compact radar cross-section measurement range," Trans. IEEE Antennas Propag., vol. 32, no. 11, pp. 12181223, Nov. 1984.

[24] V. Viikari, J. Hkli, J. Ala-Laurinaho, J. Mallat, A. V. Risnen, "A feed scanning based APC technique for compact antenna test ranges," Trans. IEEE Antennas Propag., vol. 53, no. 10, pp. 3160 3165, Oct 2005.

[25] K. R. Mahmoud, M. El-Adawy, R. Bansal, S. H. Zainud-Deen, and S. M. M. Ibrahem, "Investigating the Interaction between a Human Head and a Smart Handset for 4G Mobile Communication Systems," Progress In Electromagnetics Research C, PIERC 2, Vol. 2, 169-188, 2008.

[26] K. R. Mahmoud, M. El-Adawy, R. Bansal, S. H. Zainud-Deen, and S. M. M. Ibrahem, "MPSO-MOM: A Hybrid Modified Particle Swarm Optimization and Method of Moment Algorithm for Smart Antenna Synthesis," Electromagnetics, vol. 28, pp. 411-426, 2008.

[27] G. Jakobsson and B. Sundvall, "Low weight antenna element," WO patent WO9618219, June 13 1996.